Integrated Full Wave Analysis of RF Heating and Current Drive in Toroidal Plasmas

A. Fukuyama 1), S. Murakami 1), A. Sonoda 1), M. Honda 1)

1) Graduate School of Engineering, Kyoto University, Kyoto, Japan

email contact of main author: fukuyama@nucleng.kyoto-u.ac.jp

Abstract. Self-consistent and sufficiently accurate modeling of wave-plasma interactions is one of the key issues in producing and sustaining burning plasmas. We have carried out self-consistent full wave analysis taking account of the modification of momentum distribution functions by using the integrated modeling code TASK [1]. Integral formulation of the self-consistent full wave analysis was developed to include the finite gyroradius effects indispensable for describing the behavior of electron Bernstein waves and absorption of ICRF waves by energetic ions.

1. Introduction

Self-consistent and sufficiently accurate modeling of wave-plasma interactions is one of the key issues in producing and sustaining burning plasmas. We have carried out self-consistent full wave analysis taking account of the modification of momentum distribution functions by using the integrated modeling code TASK [1]. Integral formulation of the self-consistent full wave analysis was developed to include the finite gyroradius effects indispensable for describing the behavior of electron Bernstein waves and absorption of ICRF waves by energetic ions.

2. Modification of momentum distribution

Preferential interaction with waves generates fast ions in ICRF heating and energetic electrons in current drive. Quasilinear diffusion in momentum space flattens the distribution function $f(\boldsymbol{p})$ and generate fast particles. These modifications of $f(\boldsymbol{p})$ affect the absorption of the wave and modify the spatial structure of wave amplitude. Therefore self-consistent analysis of wave propagation and momentum distribution function is required to describe RF heating and current drive. In the case of ECRF current drive, such a self-consistent analyses have been carried out using the ray tracing method. We have now applied it to the full wave analysis of ICRF and Alfén waves.

The integrated code TASK [1] includes a full wave module WM, a wave dispersion module DP, and a Fokker-Planck module FP. WM solves Maxwell's equation in magnetic surface coordinates with a dielectric tensor calculated by DP. DP evaluates the kinetic dielectric tensor by numerical integration for momentum distribution functions calculated by FP. FP solves the Fokker-Planck equation on each magnetic surface with quasilinear diffusion evaluated by bounce averaging the wave electric field calculated by WM. Fig. 1 illustrates a result of self-consistent analysis of minority ion heating. We have observed broadening of the power deposition profile due to the fast ion tail formation. Systematic analysis for ITER configuration will be reported.

3. Full wave analysis of electron cyclotron waves in ST

In a spherical tokamak (ST) configuration, central heating by ECRF waves is prevented by cutoff layers due to high density and cyclotron harmonics layers due to low aspect ratio. In

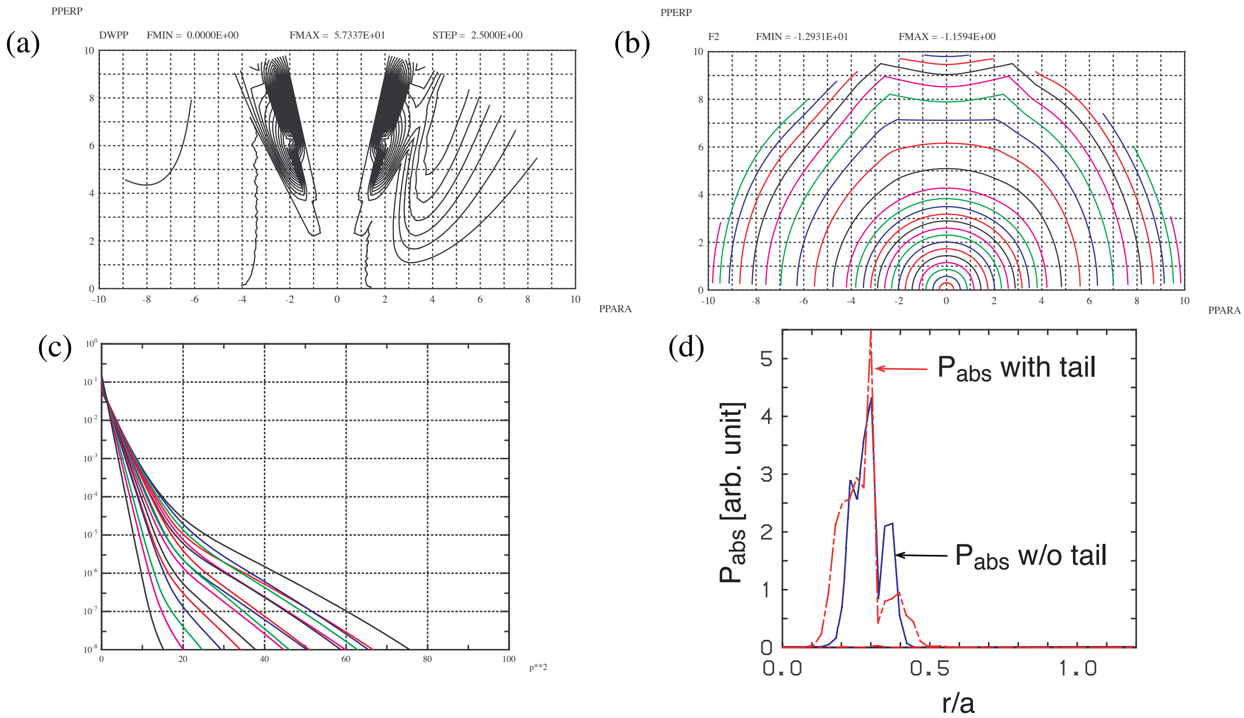

FIG. 1. heating: (a) bounce averaged quasilinear diffusion coefficient in momentum space, (b) contours of momentum distribution function, (c) formation of fast ion tail in $f(p)$, (d) power deposition profile with and without fast ion tail.

order to describe the penetration over the cutoff layer, full wave analysis is necessary. We have employed TASK/WM to describe the extraordinary wave in a small-size ST configuration similar to the LATE [2].

Fig. 2 shows the poloidal structure of the wave ($f = 2.8\,\mathrm{GHz}$, toroidal mode number $n = 16$, $B = 0.0552\,\mathrm{T}$, $n_e(0) = 10^{17}\,\mathrm{m}^{-3}$, $\nu/\omega = 10^{-3}$). The wave is launched from the low field side and propagates across the right-hand cutoff surface located halfway between the upper hybrid surface and the plasma surface. After tunneling the evanescent layer, a part of the wave is converted to a short-wavelength slow wave which propagates along the upper hybrid surface. The plasma cutoff surface also exists near the magnetic axis. At the upper hybrid surface, the radial electric field becomes very strong and the wave power is absorbed through collisional damping in a low temperature plasma. The absorption mechanism of cutoff-resonance-cutoff triplet is clearly described.

In a high temperature plasma, the slow wave is mode-converted to the electron Bernstein wave (EBW). The description of EBW requires finite gyroradius effects which is not included in the present analysis. The analysis in a tokamak plasma with a larger size and a stronger magnetic field will require massively parallel computation.

4. Integral formulation of finite gyroradius effects

In order to describe the ICRF in the presence of fast ions or with higher harmonics as well as EBW, the finite gyroradius effects has to be taken into account. The analysis with differential operators is usually limited up to the second order harmonics and not applicable for $k_\perp\rho \gtrsim 1$. The approach in three-dimensional Fourier space requires very large computer resources. We

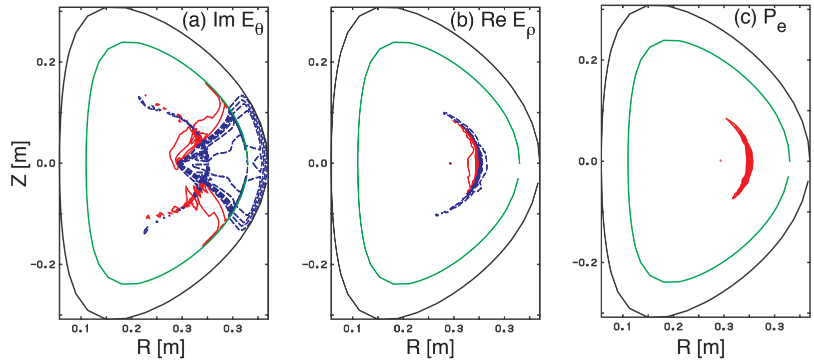

FIG. 2. Full wave analysis of electron cyclotron waves in a small-size spherical tokamak: (a) poloidal electric field, (b) radial electric field, (c) power absorption by electrons near the upper hybrid layer.

$10^{17}\ \mathrm{m}^{-3}$ $\quad 2\times10^{17}\ \mathrm{m}^{-3}$ $\quad 3\times10^{17}\ \mathrm{m}^{-3}$ $\quad 4\times10^{17}\ \mathrm{m}^{-3}$ $\quad 5\times10^{17}\ \mathrm{m}^{-3}$

(a)

(b)

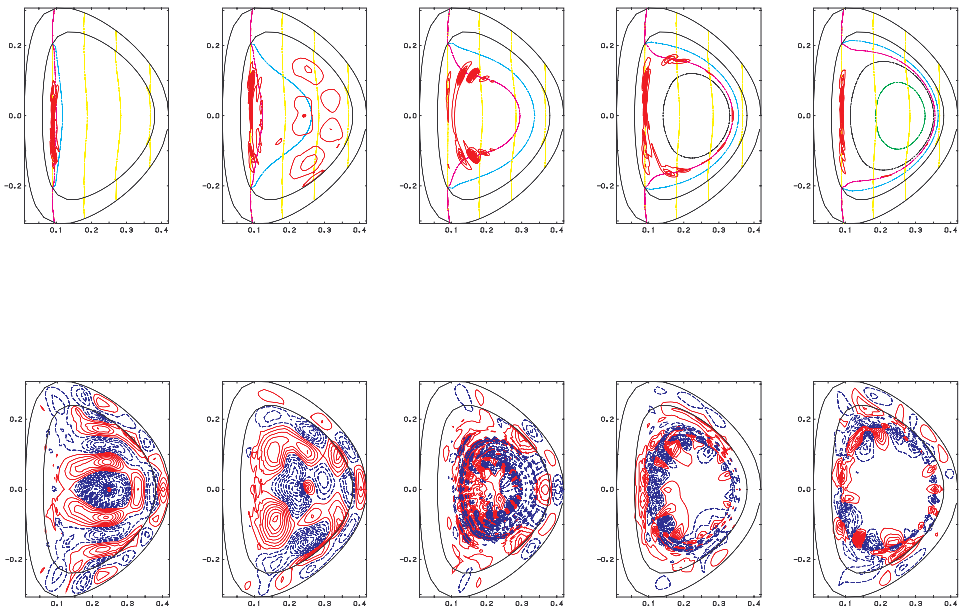

FIG. 3. Density dependence of electron cyclotron wave propagation and absorption. (a) poloidal electric field and (c) power absorption by electrons.

have formulated the integral representation of the dielectric tensor, symbolically written as

$$\nabla\times\nabla\times\boldsymbol{E}(\boldsymbol{r}) - \frac{\omega^2}{c^2}\int \mathrm{d}\boldsymbol{r}_0 \int \mathrm{d}\boldsymbol{r}'\boldsymbol{K}_1(\boldsymbol{r},\boldsymbol{r}',\boldsymbol{r}_0)\frac{\partial f_0(\boldsymbol{p}',\boldsymbol{r}_0)}{\partial \boldsymbol{p}'}\cdot\boldsymbol{E}(\boldsymbol{r}') = \mathrm{i}\,\omega\mu_0\boldsymbol{j}_{\mathrm{ext}} \tag{1}$$

where $\boldsymbol{r}_0$ is the gyrocenter position. We have obtained an explicit expression of the kernel $\boldsymbol{K}_1$ for a plasma with the Maxwellian distribution. The one-dimensional analysis in a slab plasma reproduces the results by Sauter et al. [3]. The two dimensional analysis in a tokamak configuration is under way. The integral approach should be extended to the quasilinear operator in the Fokker-Planck analysis for consistency. The operator may be expressed as

$$\frac{\partial f_0(\boldsymbol{p},\boldsymbol{r}_0,t)}{\partial t}+\left(\frac{\partial f_0}{\partial \boldsymbol{p}}\right)_{\boldsymbol{E}}+\frac{\partial}{\partial \boldsymbol{p}}\int \mathrm{d}\boldsymbol{r}\int \mathrm{d}\boldsymbol{r}'\,\boldsymbol{K}_2(\boldsymbol{r},\boldsymbol{r}',\boldsymbol{r}_0)\cdot\boldsymbol{E}(\boldsymbol{r})\,\boldsymbol{E}(\boldsymbol{r}')\cdot\frac{\partial f_0(\boldsymbol{p}',\boldsymbol{r}_0,t)}{\partial \boldsymbol{p}'}=\left(\frac{\partial f_0}{\partial \boldsymbol{p}}\right)_{\mathrm{col}} \quad (2)$$

The kernels $\boldsymbol{K}_1$ and $\boldsymbol{K}_2$ are closely related and localized in the region $|\boldsymbol{r}-\boldsymbol{r}_0| \lesssim \rho$ and $|\boldsymbol{r}'-\boldsymbol{r}_0| \lesssim \rho$. Formulation of explicit expression is also reported.

This work is supported by Grant-in-Aid for Scientific Research from JSPS and Grant-in-Aid for Specially Promoted Research from MEXT.

References

[1] FUKUYAMA A et al., Proc. of 20th IAEA Fusion Energy Conf. (Villamoura, Portugal, 2004) IAEA-CSP-25/CD/TH/P2-3.
[2] MAEKAWA T et al., Proc. of 20th IAEA Fusion Energy Conf. (Villamoura, Portugal, 2004) IAEA-CSP-25/CD/EX/P4-27.
[3] SAUTER O, Vaclavik J, Nucl. Fusion **32** (1992) 1455.